Reaction rate of a composite core-shell nanoreactor with multiple, spatially distributed embedded nano-catalysts

Marta Galanti[a,b], **Duccio Fanelli**[b], **Stefano Angioletti-Uberti**[c], **Matthias Ballauff**[d,e], **Joachim Dzubiella**[*d,e] **and Francesco Piazza**[*a]

We present a detailed theory for the total reaction rate constant of a composite core-shell nanoreactor, consisting of a central solid core surrounded by a hydrogel layer of variable thickness, where a given number of small catalytic nanoparticles are embedded at prescribed positions and are endowed with a prescribed surface reaction rate constant. Besides the precise geometry of the assembly, our theory accounts explicitly for the diffusion coefficients of the reactants in the hydrogel and in the bulk as well as for their transfer free energy jump upon entering the hydrogel shell. Moreover, we work out an approximate analytical formula for the overall rate constant, which is valid in the physically relevant range of geometrical and chemical parameters. We discuss in depth how the diffusion-controlled part of the rate depends on the essential variables, including the size of the central core. In particular, we derive some simple rules for estimating the number of nanocatalysts per nanoreactor for an efficient catalytic performance in the case of small to intermediate core sizes. Our theoretical treatment promises to provide a very useful and flexible tool for the design of superior performing nanoreactor geometries and with optimized nanoparticle load.

1 Introduction

In recent years, metallic nanoparticles have emerged as potent catalysts for various applications[1,2]. In particular, the discovery that gold becomes a catalyst when divided to the nanophase has led to an intense research in this field[3,4]. In many cases the synthesis and the catalytic applications must be handled in the liquid phase, mostly in water. Secure handling of nanoparticles in a liquid phase can be achieved by polymeric carriers that have typical dimensions in the colloidal domain. Examples thereof include dendrimers[5,6] or spherical polyelectrolyte brushes[7]. Such systems allow one to generate nanoparticles in aqueous phase in a well-defined manner and handle them securely in catalytic reactions.

More recently, thermosensitive colloidal microgels have been used as carriers for metallic nanoparticles in catalysis[8]. Fig. 1 displays the scheme of such a carrier system that may be regarded as a nanoreactor: a thermosensitive network composed of cross-linked chains of poly(N-isopropylacrylamide) (PNIPAM) has been attached to a solid core made of an inert material as, *e.g.*, polystyrene or silica[9]. Metal nanoparticles are embedded in the network which is fully swollen in cold water. Raising the temperature above the critical temperature (32° C for PNIPAM), a volume transition takes place within the network and most of the water is expelled[8]. Lu *et al.*[9] have been the first to show that the catalytic activity of the embedded nanoparticles is decreased when shrinking the network by raising the temperature. This effect has been explained by an increased diffusional resistance mass transport within the shrunk network[8,9]. A similar model has been advanced by Carregal-Romero *et al.* when considering the catalytic activity of a single gold nanoparticle embedded concentrically in a PNIPAM-network[10].

Recently, we have shown that the mobility of reactants is not the only important factor: an even larger role is played by the change of polarity of the network when considering mass transport from bulk to the catalyst(s) through such medium[11,12]. This theory is based on the well-known seminal paper by Debye[13] and considers a single nanoparticle located in the center of a hollow thermosensitive network[12]. Here, the substrate that reacts at the surface of the nanoparticle diffuses through a free-energy landscape created by the hydrogel environment. In other words, the reactants experience a change in the solvation free energy when entering the gels from bulk solvent, which can be equally regarded as an sorption free energy or *transfer* free energy. For instance, the free energy of a substrate may be lowered upon entering the network. In this way

a Université d'Orléans, Château de la Source, 45100, Orléans, France, Centre de Biophysique Moléculaire, CNRS-UPR4301, Rue C. Sadron, 45071, Orléans, France.
b Università degli Studi di Firenze, Dipartimento di Fisica e Astronomia and CSDC, via G. Sansone 1, IT-50019 Sesto Fiorentino, Firenze, Italia.
c International Center for Soft Matter Research, Beijing University of Chemical Technology, Beijing 100029, China.
d Institut für Physik, Humboldt-University Berlin, 12489 Berlin, Germany.
e Institut für Weiche Materie und Funkionale Materialien, Helmholtz-Zentrum Berlin, 14109 Berlin, Germany.

the number of substrate molecules in the network will be augmented, so that their increased concentration in the vicinity of the catalyst will lead to a higher reaction rate. The free-energy change $\Delta G \stackrel{\text{def}}{=} G_{\text{in}} - G_{\text{out}}$ for the substrate outside and inside the network leads to a Nernst distribution for the substrate's concentration within the system. This effect offers a new way to manipulate the catalytic activity and selectivity of metallic nanoparticles [11].

In this paper we formulate a more general theory, that is able to account for the geometry of core-shell nanoreactors featuring *many* catalysts, as shown schematically in Fig. 1. Here, a given number N of catalytic centers are encapsulated randomly in a network. We calculate the total rate of the catalytic reaction for a prescribed geometry of the catalysts, given values of N and ΔG and specified diffusion constants for the substrate in the bulk and in the network. The rate constant computed in this way can be compared to that characterizing an equal number of particles suspended freely in solution. The present model has been designed to describe the well-studied core-shell systems [8,9], but is equally adapted to the study of systems where catalytic centers are embedded in homogeneous microgels [14]. Up to now, most of the experimental work has been done using the reduction of 4-nitrophenol by borohydride ions in aqueous solution [15,16]. This reaction can be regarded as a model reaction [17], since it can be monitored with high precision thus leading to very accurate kinetic data. The rate-determining step proceeds at the surface of the nanoparticles and the mechanism is known [18]. The present theory, however, comprises also the nanoreactors in which enzymes are used as catalytic centers embedded in the network shell [19].

In general, diffusion-influenced reactions (DIR) are ubiquitous in many contexts in physics, chemistry and biology [20–23]. However, while the mathematical foundations for the description of DIR in simple systems have been laid nearly a century ago [13,24,25], many important present-day problems, including the catalytic activity of composite core-shell nanoreactors, require considering complex geometries and multi-connected reactive boundary systems. The first attempts to consider DIR featuring many competing sinks date back to the 1970s [26,27], while more sophisticated methods have been developed subsequently to deal with arbitrary systems comprising many partially reactive boundaries [28–30]. Along similar lines, the theory developed in this paper, based on general results proved in Ref. [29], provides a novel, accurate description of DIR occurring between a small substrate molecule and the catalytic centers embedded in a large, composite nanoreactor system.

Our theory is fully general, in that it covers the whole spectrum of rate-limiting steps in catalysis, from reaction-limited to diffusion-limited reactions. While the theory allows one to compute the reaction rate for an arbitrary catalytic surface turnover rate, closed-form analytical expression are derived for strongly reaction-limited and diffusion-limited reac-

tions. In the limit of a dilute random distribution of NPs encapsulated in a thick hydrogel shell, we find that the overall diffusion-controlled rate constant of our core-shell composites is described by a Langmuir-like isotherm of the form

$$\frac{k}{k_S} = \frac{N\varepsilon\zeta e^{-\beta\Delta G}}{1 + N\varepsilon\zeta e^{-\beta\Delta G}} \quad (1)$$

where N is the number of nanoparticles, $\zeta = D_i/D_o$ is the ratio of the diffusion constants in the hydrogel (i for inner) and bulk (o for outer), $\varepsilon = a/R_0 \ll 1$ is the ratio of NP size (radius) to the nanoreactor size and $k_S = 4\pi D_o R_0$ is the Smoluchowski rate constant for the nanoreactor as a whole, *i.e.* the total flux (in units of bulk substrate concentration) of substrate molecules to a stationary perfectly absorbing sink of size R_0 in the bulk. The above expression is valid for small sizes of the central core. Interestingly, for configurations where the core size becomes of the same order of the whole composite (thin shell), our theory shows that in general the rate constant is increased, up to 40 %, depending on the transfer free energy jump and on the reactant mobility in the shell.

In the limit of slow surface substrate-product conversion rate, i.e. for reaction-limited kinetics, we find that

$$k \simeq Nk^* e^{-\beta\Delta G} + \mathcal{O}[(k^*/k_S^+)^2] \quad (2)$$

where k^* is the intrinsic turnover rate constant that describes the transformation of substrate to product molecules at the nanocatalyst surface (units of inverse concentration times inverse time). This means that when the surface substrate conversion rate constant is weak, the geometrical features of the overall assembly and the mobility of substrate molecules within the hydrogel shell become immaterial. In this case, the crucial control parameter is the transfer free energy jump.

The paper is organized as follows. In section 2 we describe our mathematical model and pose the associated boundary-value problem. In section 3, we describe concisely the procedure that leads us to the exact solution of the posed problem (the mathematical details can be found in the appendix). Section 4 illustrates an analytic approximation that provides an extremely good description of the exact solution for small core sizes in the physically relevant range of parameters. In particular, we discuss how this formula can be used to derive practical criteria to design nanoreactors with optimized performances. Finally, we wrap up our main results in section 5.

2 Core-shell model and defining equations

We model a core-shell nanoreactor consisting of a polystyrene (PS) core surrounded by a microgel layer as two concentric spheres centered at the origin of a Cartesian $3D$ frame, as depicted in Fig. 1. We denote with R_S and R_0 the core and
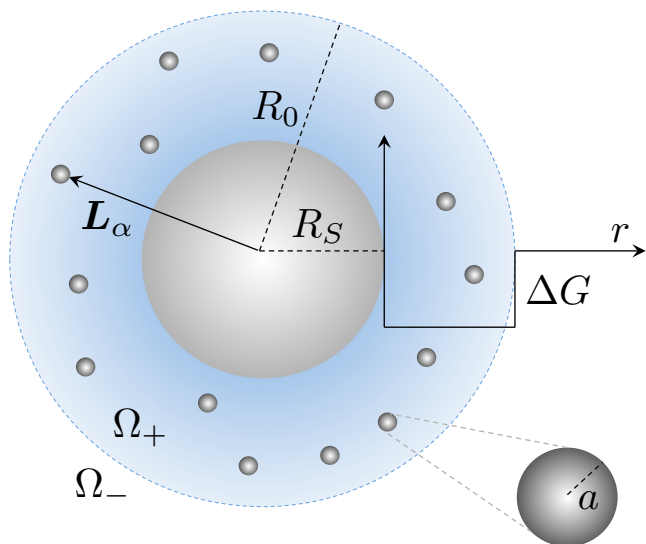
Fig. 1 Scheme of a core-shell nanoreactor of radius R_0 containing $N+1$ spheres: the solid polystyrene (PS) core (radius R_S) is shown at the center, along with N catalytic nanoparticles of radius a at positions $\mathbf{L}_\alpha$ ($\alpha = 2, 3, \ldots, N+1$). The internal (microgel) domain Ω_+ (with reactant diffusion coefficients D_i) and the external (bulk solution) domain Ω_- (with reactant diffusion coefficients D_o) are indicated explicitly, together with a schematic free-energy radial profile showing the transfer free-energy jump ΔG. In our treatment the latter can be both repulsive, $\Delta G > 0$, or attractive, $\Delta G < 0$.

shell radius, respectively. The shell is assumed to be a homogeneous continuum, carrying N small nano-catalysts (metal nanoparticles or enzymes) that we model as spheres of radius a. For the sake of simplicity, and in accordance to our general multi-sink theory [31], we label the PS core as the inner sphere with $\alpha = 1$ and position vector $L_1 = 0$ and denote the position of the N nanocatalysts with the vectors L_α, $\alpha = 2, 3, \ldots, N+1$. We want to compute the total reaction rate constant for reactions where a substrate (or ligand) molecule is converted to some product species at the surface of the catalyst spheres. These are endowed with a surface rate constant k^*, which is in general a function of temperature due to underlying thermally activated surfaces processes. Let us denote with $\mathscr{S}_0 \equiv \{r_0, \theta_0, \varphi_0\}$ the reference frame with the origin at the nanoreactor center and with $\mathscr{S}_\alpha \equiv \{r_\alpha, \theta_\alpha, \varphi_\alpha\}$ the N reference frames with the origins at the nanospheres centers and the axes parallel to $\mathscr{S}_0$ (of course $\mathscr{S}_1 \equiv \mathscr{S}_0$). This formally defines the following 3D domains

$$\begin{aligned}
\Omega^+ &= \{r_0 \in (0, R_0], \theta_0 \in [0, \pi], \varphi_0 \in (0, 2\pi]\} \setminus \cup_\alpha \Omega_\alpha \\
\Omega^- &= \{r_0 \in [R_0, \infty), \theta_0 \in [0, \pi], \varphi_0 \in (0, 2\pi]\}
\end{aligned} \quad (3)$$

where $\Omega_1 = \{|r_0| < R_S\}$ denotes the interior of the PS core and $\Omega_\alpha = \{|r_\alpha| = |r_0 - L_\alpha| < a\}$, $\alpha = 2, 3, \ldots, N+1$, denote

the interior of the α-th nanosphere. The reactant diffuses with diffusion coefficients D_i and D_o inside the microgel shell and in the bulk, respectively. In general one can assume $D_i < D_o$ due to obstructed or hindered diffusion in the microgel [32].

2.1 Steady-state boundary-value problem

Let ρ_B denote the bulk density of reactants and let us introduce the time-dependent normalized density $u(r,t) = \rho(r,t)/\rho_B$. We assume that the system relaxation time for the diffusive flux of B particles (the reactants), $t_D \simeq (R_0 - R_S)^2/D_i$, is small enough to neglect time-dependent effects. Hence, in the absence of external forces, the diffusion of reactants with normalized number density $u(r)$ is described by the steady-state diffusion equation

$$\nabla \cdot [D(r)\nabla u(r)] = 0 \qquad \text{in } \Omega = \Omega^+ \cup \Omega^- \quad (4)$$

with

$$D(\mathbf{r}) = \begin{cases} D_i & \text{in} \quad \Omega^+ \quad \text{(microgel)} \\ D_o & \text{in} \quad \Omega^- \quad \text{(bulk)} \end{cases} \quad (5)$$

and which should be solved with the customary bulk boundary condition

$$\lim_{|r| \to \infty} u(r) = 1 \quad (6)$$

It is well known from the general theory of partial differential equations that the classical solution (twice continuously differentiable in Ω and continuous on $\overline{\Omega}$) of the stationary diffusion equation (4) does not exist in the whole domain Ω [33]. Therefore one should consider the function

$$u(r) = \begin{cases} u^+(r) & \text{in} \quad \Omega^+ \quad \text{(microgel)} \\ u^-(r) & \text{in} \quad \Omega^- \quad \text{(bulk)} \end{cases} \quad (7)$$

Accordingly, we should impose a condition for the substrate concentration field at the bulk/microgel interface, $\partial \Omega_0 \equiv \{r_0 = R_0\}$. It has been demonstrated recently that a key factor controlling the overall reaction rate is the transfer free-energy jump ΔG, a quantity that describes the partitioning of the reactant in the microgel versus bulk [12]. For a single nanocatalyst at the nanoreactor center, a free-energy jump at the solvent-microgel interface can be accounted for through a modified reactant density in the microgel, namely $\rho \to \rho \exp(-\beta \Delta G)$ when crossing the bulk/microgel interface. This is also the case for many catalysts in the infinite dilution limit. Here we assume that such description is a valid approximation for realistic nanoreactors, where the nanocatalyst packing fraction is indeed very small, as discussed in depth later. Accordingly, we require

$$(u^+ - \lambda u^-)\big|_{\partial \Omega_0} = 0 \quad (8)$$

where $\lambda = \exp(-\beta \Delta G)$, $\beta = 1/k_B T$ being the inverse temperature. Furthermore, the following continuity condition for

the local diffusion fluxes should also hold at the bulk/microgel interface

$$\left(\frac{\partial u^-}{\partial r_0} - \zeta \frac{\partial u^+}{\partial r_0}\right)\bigg|_{\partial \Omega_0} = 0 \qquad (9)$$

where we have introduced the diffusion anisotropy parameter

$$\zeta = \frac{D_i}{D_o} \qquad (10)$$

Finally, reflecting boundary conditions should hold at the surface of the inert PS core, *i.e.*

$$\frac{\partial u^+}{\partial r_0}\bigg|_{r_0 = R_S} = 0 \qquad (11)$$

2.2 The reaction rate constant

We are interested in the pseudo-first-order irreversible diffusion-influenced reaction between the N nano-catalysts C encapsulated in the microgel and reactants B freely diffusing in the bulk and in the microgel

$$C + B \underset{k_{-D}}{\overset{k_D}{\rightleftharpoons}} C \cdot B \overset{k^*}{\rightarrow} C + P \qquad (12)$$
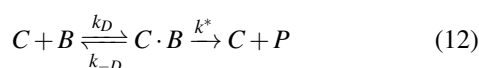
where $C \cdot B$ denotes the so-called *encounter complex*, k_D and k_{-D} are the association and dissociation diffusive rate constants, respectively, and k^* is the surface rate constant of the chemical reaction occurring at the reactive catalysts' boundaries. Reactions of the kind (12) are customary dealt with by enforcing radiation boundary conditions * at the reaction surfaces $\partial \Omega_\alpha$, $\alpha = 2, 3, \ldots, N+1$ [25], *i.e.*

$$\left[4\pi a^2 D_i \frac{\partial u^+}{\partial r_\alpha} - k^* u^+\right]_{\partial \Omega_\alpha} = 0 \qquad \alpha = 2, 3, \ldots, N+1 \quad (13)$$

Thus, we can consider that the nanoreactors effectively act as sinks of infinite capacity according to the pseudo-first-order reaction scheme

$$C + B \overset{k}{\rightarrow} C + P \qquad (14)$$
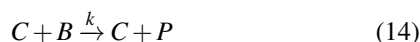
where the forward diffusion-influenced rate constant k (*i.e.* the equivalent of the measured rate constant k_{obs} [12]) is defined by the formula

$$k = \sum_{\alpha=2}^{N+1} \int_{\partial \Omega_\alpha} D_i \frac{\partial u^+}{\partial r_\alpha}\bigg|_{\partial \Omega_\alpha} dS \qquad (15)$$

Using this rate constant one can approximately describe the kinetics of the effective reaction (14) as

$$c_B(t) = c_B(0) \exp(-kct) \qquad (16)$$

---

* This kind of boundary conditions are also known as Robin boundary conditions.

where $c = const$ is the volume concentration of nanocatalysts within the microgel and $c_B(t)$ is the time-dependent effective bulk concentration of ligands. We stress that our schematization of the problem holds under the *excess reactant* condition $c \ll \rho_B$. Our goal is to compute the rate constant k defined in Eq. (15).

Equation (4) with the boundary conditions (6), (8), (9), (11) and (13) completely specify our mathematical problem. It is expedient in the following to use the dimensionless spatial variables $\xi_0 = r_0/R_0$, $\xi_1 = r_0/R_S$ and $\xi_\alpha = r_\alpha/a$ for $\alpha = 2, 3, \ldots, N+1$. Hence, our problem can be cast in the following form

$$\nabla^2 u^\pm = 0 \quad \text{in } \Omega^\pm \qquad (17a)$$

$$\left(\frac{\partial u^+}{\partial \xi_\alpha} - h u^+\right)\bigg|_{\partial \Omega_\alpha} = 0 \quad \alpha = 2, 3, \ldots, N+1 \qquad (17b)$$

$$\lim_{\xi_0 \to \infty} u^-(\xi_0) = 1 \qquad (17c)$$

$$\frac{\partial u^+}{\partial \xi_1}\bigg|_{\xi_1 = 1} = 0 \qquad (17d)$$

$$\left(u^+ - \lambda u^-\right)\big|_{\partial \Omega_0} = 0 \qquad (17e)$$

$$\left(\zeta \frac{\partial u^+}{\partial \xi_0} - \frac{\partial u^-}{\partial \xi_0}\right)\bigg|_{\partial \Omega_0} = 0 \qquad (17f)$$

The parameter

$$h = \frac{k^*}{4\pi D_i a} \equiv \frac{k^*}{k_S^+} \qquad (18)$$

gauges the *character* of the reaction. Here we have introduced the Smoluchowski rate constant for a nanocatalyst embedded in the microgel, $k_S^+ = 4\pi D_i a$. The limit $h \to \infty$ corresponds to considering the boundaries $\partial \Omega_\alpha$ as perfectly absorbing sinks. In this case the reaction (12) becomes *diffusion-limited*, as the chemical conversion from the encounter complex $C \cdot B$ to the product P becomes infinitely fast with respect to the diffusive step leading to the formation of $C \cdot B$. Otherwise, for $h \ll 1$, the chemical conversion step is slow enough compared to diffusion, which makes the reaction overall reaction-limited.

3 Exact solution of the problem and approximate analytical treatment

We look for solutions for the stationary density of reactants in the bulk and in the microgel as linear combinations of regular and irregular harmonics. Given the multi-connected structure of the boundary manifold $\cup_\alpha \Omega_\alpha$, we must consider as many *local* Cartesian reference frames as there are non-concentric

boundaries. Thus, we can look for solutions in the form

$$
u^+(r) = \sum_{\ell=0}^{\infty} \sum_{m=-\ell}^{\ell} A_{m\ell} \xi_0^{\ell} Y_{m\ell}(r_0) + \sum_{\alpha=1}^{N+1} \sum_{\ell=0}^{\infty} \sum_{m=-\ell}^{\ell} \frac{B_{m\ell}^{\alpha}}{\xi_\alpha^{\ell+1}} Y_{m\ell}(r_\alpha)
$$
(19a)

$$
u^-(r) = 1 + \sum_{\ell=0}^{\infty} \sum_{m=-\ell}^{\ell} E_{m\ell} \xi_0^{-\ell-1} Y_{m\ell}(r_0)
$$
(19b)

where $Y_{mn}(r)$ are spherical harmonics, $\xi_0 = r_0/R_0$, $\xi_1 = r_0/R_S$, $\xi_\alpha = r_\alpha/a$ for $\alpha = 2, 3, \ldots, N$ and A_{mn}, B_{mn}^{α} and E_{mn} are $N+3$ infinite-dimensional sets of unknown coefficients that can be determined by imposing the boundary conditions (17b) and (17d) and the pseudo-continuity conditions at the microgel-solvent interface, eqs (17e) and (17f). This can be done straightforwardly using known addition theorems for spherical harmonics, which results in an infinite-dimensional linear system of equations for the unknown coefficients (see

appendix A for the details). Furthermore, making use of known properties of solid spherical harmonics, it is easy to see that the rate constant defined by Eq. (15) is simply given by

$$
k = -k_S^+ \sum_{\alpha=2}^{N+1} B_{00}^{\alpha}
$$
(20)

As shown in the appendix A, the exact solution to the steady-state problem (17) can be worked out in principle to any desired precision by keeping an appropriate number of multipoles. Remarkably, a simple yet accurate *analytical* expression can be easily obtained in the monopole approximation (MOA), which corresponds to keeping only the $\ell = 0$ term in the multipole expansions (19)[26,27]. In particular, it is interesting to compute the rate normalized to the Smoluchowski rate of an isolated sink of the same size as the whole nanoreactor in the bulk, *i.e.* $k_S^- = 4\pi D_0 R_0$. We obtain (see appendix B for the details)

$$
\frac{k}{k_S^-} = N k^* \left(\frac{a}{R_0} \right) \frac{\zeta e^{-\beta \Delta G}}{k_S^+ + k^* \left[1 + (N-1) \left\langle \frac{a}{L_{\alpha\beta}} \right\rangle - \frac{Na}{R_0} \left(1 - \zeta e^{-\beta \Delta G} \right) \right]}
$$
(21)

where we recall that $\zeta = D_i/D_0$ and $k_S^+ = 4\pi D_i a$. This is the key analytical result derived in this work, that can be readily employed to predict and optimize the geometry and activity of typical core-shell nanoreactors. The quantity $\langle a/L_{\alpha\beta} \rangle$ stands for the average inverse inter-catalyst separation. This can be computed analytically under the reasonable assumption that spatial correlations in the catalysts configurations are negligible (see appendix B),

$$
\left\langle \frac{a}{L_{\alpha\beta}} \right\rangle = \frac{2(1-\varepsilon)^5 - 5(1-\varepsilon)^2(\gamma+\varepsilon)^3 + 3(\gamma+\varepsilon)^5}{(1-\varepsilon)^6 - 2(1-\varepsilon)^3(\gamma+\varepsilon)^3 + (\gamma+\varepsilon)^6} \left(\frac{3a}{5R_0} \right)
$$
$$
:= \varepsilon C(\varepsilon, \gamma)
$$
(22)

where $\gamma = R_S/R_0$ denotes the fraction of the nanoreactor size occupied by the PS core and $\varepsilon = a/R_0$ is the non-dimensional size of each catalyst. We see that, since $\varepsilon \ll 1$, one has $1 + \varepsilon/3 \lesssim C \lesssim 6(1+\varepsilon)/5$, *i.e.*, C is of the order of unity, $1.005 \lesssim C \lesssim 1.217$ (taking $\varepsilon \approx 0.0146$ from experiments[34]).

In the limit of vanishing surface reactivity of the embedded nano-catalysts it is immediate to show from eq. (21) that

$$
k \simeq N k^* e^{-\beta \Delta G} + \mathcal{O}[(k^*/k_S^+)^2]
$$
(23)

We see that, if the surface substrate conversion rate constant is weak, this becomes the rate-limiting step for the overall rate of the nanoreactor, irrespective of the geometrical features of

the assembly and of the mobility properties of the hydrogel shell. In this case, it becomes crucial to control the transfer free energy jump to tune the rate of the composite nanoreactor. Conversely, if the catalytic action exerted by the metal nanoparticles encapsulated in the microgel is fast with respect to diffusion, *i.e.* $k^* \gg k_S^+$, expression (21) can be simplified by taking the limit $k^* \to \infty$. This yields the expression for the fully diffusion-controlled rate

$$
\frac{k}{k_S^-} = \frac{N \varepsilon \zeta e^{-\beta \Delta G}}{1 + (N-1)\varepsilon C(\varepsilon, \gamma) - N\varepsilon \left(1 - \zeta e^{-\beta \Delta G} \right)}
$$
(24)

which we will discuss in depth in the following section. Note that for $N = 1$ Eq. (24) coincides with the solution of the Debye-Smoluchowski problem[13] for a single perfectly absorbing sink located at the center of the shell, with $G(r) = \{\Delta G$ for $a < r \leq R_0 | 0$ for $r > R_0\}$.

Formulas (21) and (24) have been derived in the monopole approximation, which means that any reflecting boundaries in the problem are not taken into account. Therefore, these should be used to approximate the rate constant of a composite nanoreactor for small to moderate sizes of the central PS core. In the following sections, we provide a thorough characterization of the rate constant of a composite core-shell nanoreactor, computed exactly by solving Eqs. (31), and we compare it to

the approximate MOA analytical expression (24) in the physically relevant diffusion-limited regime ($k^* \to \infty$).

4 The diffusion-controlled regime

We now discuss in more detail the essential features of the diffusion-controlled rate in Eq. (24). In the monopole approximation, valid for small to intermediate sizes of the central reflecting (inert) core, the role of the latter only enters indirectly through the spatial average $\langle a/L_{\alpha\beta}\rangle = Ca/R_0$, with $C \simeq 1$. In the swollen configuration, the central core does not occupy a large fraction of the overall nanoreactor volume, with $\gamma \approx 0.3$ (as taken from the experiments reported in Ref.[34]). Hence, in this regime we expect that the exact size of the core should not play a significant role for the diffusion-controlled rate for relevant values of the physical parameters, *i.e.*, (weak) attraction to the hydrogel $\Delta G < 0$ and decreased internal diffusion $\zeta < 1$.

In Fig. 2 we compare the approximate expression (24) to the exact solution of Eqs. (31) for two different mobility ratios $\zeta = 0.2$ and 1.0 and core size $\gamma = 0.353$ (as in previous experiments[34]). The NP size is held fixed as $\varepsilon = 0.0146$ as also provided from experiments. It is apparent that the analytical treatment is remarkably accurate in these conditions and deviates from the exact solution by less than one percent in the worst cases. This proves that our analytical treatment provides a reliable tool for realistic values of the physico-chemical and geometrical parameters. A comparison of different values of the substrate mobility within the gel (ζ), clearly highlights that all rates are higher when the ligand is more mobile within the gel shell. Concerning the overall form of the curves, one can see that the initial linear rise of the rates is followed by a saturation at large values of N. The approach to saturation is slow for small values of ΔG, but begins markedly earlier (*i.e.* for smaller N) if the sorption free energy reaches values as small as a few $k_B T$, the thermal energy. Hence, as discussed already previously, a decisive factor in the design of optimized nanoreactors must be clearly the tuning of the reactant-hydrogel interaction towards attraction. We note that free energy gains ΔG of the order of a few $k_B T$ seem utterly realistic for small hydrophilic substrates, such as nitrobenzol and nitrophenyl. For comparison, a reasonable upper bound could be estimated as the free energy jump of about 7 kT reported for the sorption of a protein into a hydrophilic network[35]. These estimates are also consistent with partitioning data of small molecules, such as acetaminophen, into PNIPAM[36], where the transfer free energy can be estimated as $\Delta G \simeq -k_B T \ln K$, where K is the partitioning coefficient.

4.1 Optimizing the number of nanocatalysts

As we see from Eq. (25) the maximum achievable rate is $k = k_S^- = 4\pi D_0 R_0$, that is, the Smoluchowski rate of a sink of size equal to that of the total nanoreactor, *i.e.* the nanoreactor should be big for high activity. In the limit of small NP to nanoreactor size ratio, $\varepsilon \ll 1$, Eq. (24) can be simplified to the following form

$$\frac{k}{k_S^-} = \frac{N\varepsilon\,\zeta e^{-\beta\Delta G}}{1+N\varepsilon\,\zeta e^{-\beta\Delta G}}. \qquad (25)$$

Let us recall the important parameters, that is, the NP to nanoreactor size ratio $0 < \varepsilon = a/R_0 \ll 1$, the number of NPs N, the scaled reactant mobility inside the shell $0 < \zeta = D_i/D_0 \lesssim 1$, and finally the transfer free energy change ΔG for the reactants upon entering the hydrogel. Clearly, if the mobility vanishes, $\zeta \ll 1$ or the free energy jump $\Delta G \gg k_B T$ is substantially repulsive, the reaction is significantly slowed down. However, in realistic systems the mobility will be certainly slowed down to some extent but not vanish. ΔG may be even negative (attractive) if the reactant interacts favorably with the polymer as found for rather hydrophobic reactants and collapsed PNIPAM-based hydrogels[11,12]. Since ΔG enters Eq. (25) exponentially, substantial effects are expected following small changes in the interaction. Together with ΔG, clearly the number of NPs and their size ratio with respect to the total nanoreactor size are the key quantities to tune. To save resources N should be small but large enough to warrant a high catalytic activity.

The behavior of Eq. (25) resembles a Langmuir-binding isotherm form. The rate as a function of N initially rises linearly with a slope $\varepsilon\zeta\exp(-\beta\Delta G)$ and finally saturates to the maximum rate $k = k_S^-$ for large values of N. For a single NP, $N = 1$ and not too attractive transfer free energy, we recover essentially the result for a yolk-shell nanoreactor $k \simeq 4\pi D_i a\exp(-\beta\Delta G)$, where a single NP is embedded in the center of a spherical hydrogel, apart from a slight modification of the target size, which is not a for the yolk-shell but R_i, the radius of the interior hollow confinement[11,12].

It is instructive to define an efficiency factor $f = k/k_S^-$ between 0 and 100 %, that quantifies the desired target efficiency of the nanoreactor. Solving Eq. (25) for N, we find

$$N_f = \left(\frac{e^{\beta\Delta G}}{\varepsilon\,\zeta}\right)\frac{f}{1-f} \qquad (26)$$

that is, for a fixed efficiency, the NP number needed to maintain it changes exponentially with the transfer free energy change. As a numerical example, let us assume reasonable values of $\zeta = 0.2$, $\varepsilon = 0.01$, and $\beta\Delta G = -1$. To obtain an efficiency of 50 %, $N_f = 184$ nanoparticle catalysts would be needed. If $\beta\Delta G = -2$, the number wold drop of a factor $1/e$
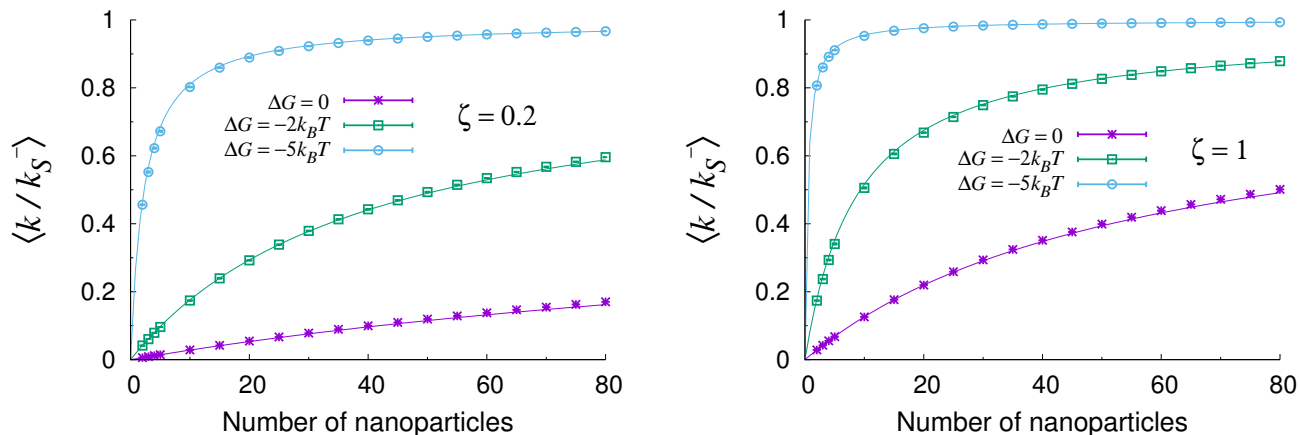
Fig. 2 Diffusion-controlled rate constant of a core-shell nanoreactor normalized to the Smoluchowski rate constant of a perfect sink of the same size, $k_S^- = 4\pi D_o R_0$ versus the number N of encapsulated nanoparticles (NP). Symbols are the exact solution of Eqs. (31) (relative accuracy of $TOL = 5 \times 10^{-4}$). Each point is an average over 10 independent configurations of the NPs (error bars smaller than the symbol size), while the solid lines are plots of the monopole approximation, Eq. (24), for the corresponding choice of parameters. The plots refer to $R_S/R_0 = 0.353$ and $a/R_0 = 0.0146$.

to $N_f = 68$. For such values of N the MOA is an excellent approximation (see Fig. 2), which makes our treatment self-consistent and sound. Note that N_f does not scale with the catalyst *surface*, as one might naively expect, rather it decreases *linearly* with the catalyst size.

Formula (26) provides a simple rule of thumb for optimizing the design and synthesis of core-shell nanoreactors for small to intermediate values of the core size. As an example, if one aims at 50 % efficiency for a relatively neutral hydrogel chemical environment ($\Delta G = 0$), where the mobility of the substrate is not significantly reduced ($\zeta = 1$), one needs to employ $N_f = 1/\varepsilon = R_0/a$ nanoparticles. For $\varepsilon = 0.01$ that would be $N_f = 100$. In the case of a polymer matrix in physical-chemical conditions leading to a reduced mobility (*e.g.* $\zeta = 0.2$), one would need five times more NPs for $\Delta G = 0$, but about the same number for $\beta\Delta G \simeq -1.6$. This clearly illustrates how the *performance* of a composite core-shell nanoreactor is non-trivially shaped by the combined action of the physical chemical properties of the hydrogel shell matrix, such as the bulk solvent-microgel transfer free energy jump and changes in translational mobility of the substrate molecules.

4.2 The role of the core size

In certain configurations, such as in the shrunk phase of thermosensitive core-shell nanoreactors past the lower critical solution temperature (LCST)[8], the core size can become comparable to the overall size of the nanoreactor. In these circumstances, the MOA breaks down and the full solution should be used instead. Fig. 3 reports an analysis of the rate con-

stant as the core sized is varied for different values of the geometrical and physico-chemical parameters. As a first observation, the plots confirm and substantiate the discussion laid out in the previous section, as it can be appreciated that the core size does not influence the overall rate until $\gamma = R_S/R_0 \lesssim 0.4$. More generally, one can recognize that the rate constant tends to increase as the shell shrinks (increasing values of R_S/R_0). The only exception is for low N and attractive transfer free energy, where a non-monotonic trend is observed (top left panel). This is a typical screening effect[37], which originates from the subtle interplay between diffusive interactions among the nanocatalysts and individual screening due the reflecting PS core. It turns out that the transfer free energy is the prime parameter that controls the increase in the rate as the PS core size increases. The more attractive the transfer free energy, the less marked the increase. Interestingly, at fixed values of ΔG, the less mobile the substrate in the shell, the more marked the rate boosting effect of the shell shrinking. Importantly, it is apparent from the plots reported in Fig. 3 that the role of the core size is reduced for loading number of the order of a few tens and small size of the nanocatalysts. All in all, these results confirm the complex intertwining of the structural, geometrical and physico-chemical features underlying the overall catalytic activity of core-shell nanoreactors.

5 Concluding remarks

In this paper we have developed a detailed theory to compute the total reaction rate of core-shell nanoreactors with multiple catalysts embedded in the shell. The theory is utterly general
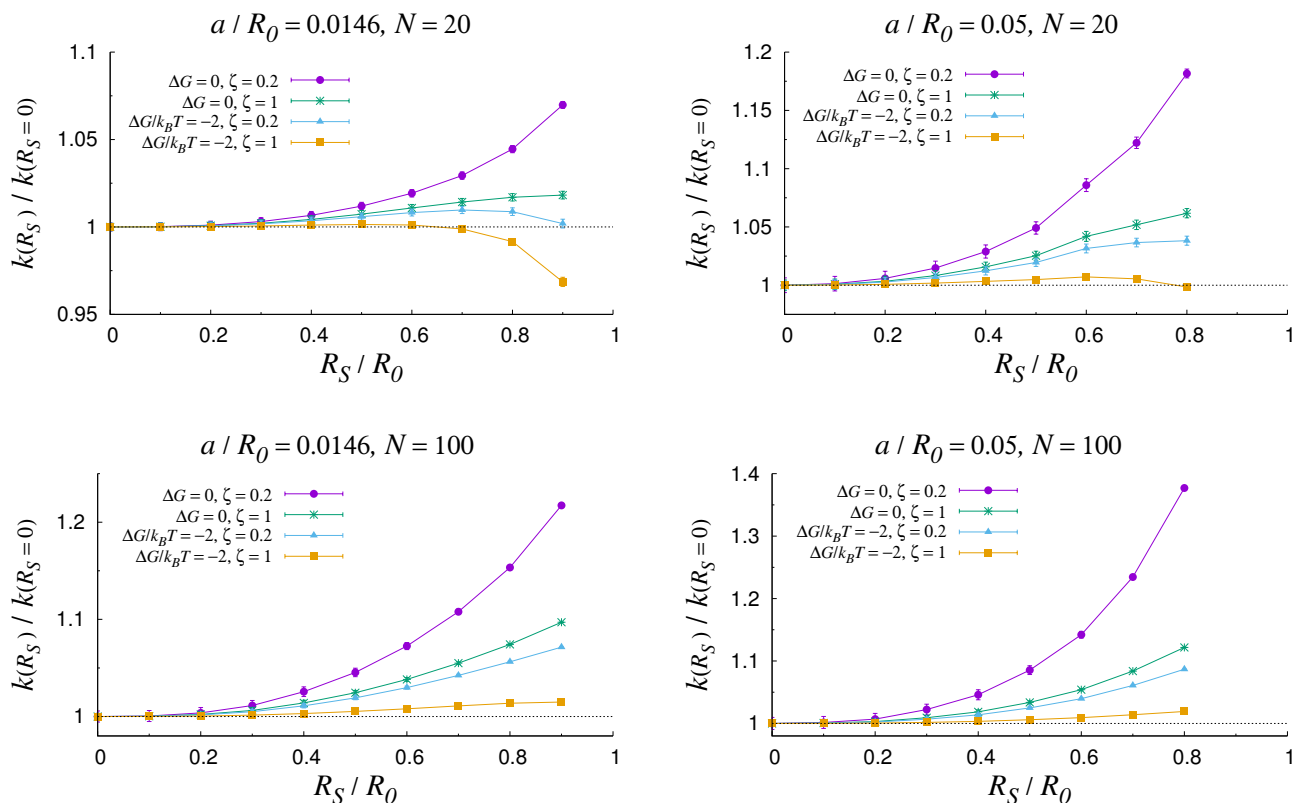
Fig. 3 Diffusion-controlled rate constant of a core-shell nanoreactor as a function of the PS core size for different values of the physico-chemical parameters and nanocatalyst loading number.

and allows one to compute the overall reaction rate to any desired accuracy for (*i*) given configuration, dimension and surface reactivity of the encapsulated nanocatalysts, (*ii*) size of the core and the shell, (*iii*) substrate mobility in the bulk and in the shell and (*iv*) transfer free-energy jump for substrate molecules. Furthermore, we computed analytical expressions in the monopole approximation that provide an excellent interpolation of the exact solution for small to intermediate sizes of the central core in the physically relevant range of parameters, *i.e.* small size and high dilution of the nanocatalysts. Our formulas supply ready-to-use simple tools that can be employed to interpret and optimize the activity of experimentally realizable nanoreactor systems. This shall be particularly useful to estimate the optimal number of embedded NPs, that should reflect a compromise between a resource-friendly design and the highest possible catalytic output. Our analytical treatment predicts an optimal number of NPs given by the following expression

$$N_f = \frac{f}{1-f} \frac{R_0}{a} \left(\frac{D_o}{D_i} \right) e^{\beta \Delta G} \qquad (27)$$

where $f \in [0, 1]$ is the desired efficiency, a and R_0 are the NP and overall nanoreactor sizes, respectively, and D_i, D_o are the substrate mobility in the shell and in the bulk, respectively. For realistic values of these parameters, one gets $N_{1/2}$ of the order of hundreds, a value for which the monopole approximation is still in excellent agreement with the exact solution for core sizes such that $R_S/R_0 \lesssim 0.4$. As discussed already previously, eq. (27) makes it clear that a decisive factor in the design of optimized hydrogel-based nanoreactors must be the tuning of the reactant-hydrogel interaction towards attraction ($\Delta G < 0$) for a specific reaction (or mix of reactions). Furthermore, as hydrogel that cause strongly reduced substrate mobility also demand more NPs to achieve high efficiency ($N_f \propto D_o/D_i$), the choice of the shell hydrogel should be made so as to privilege smooth longer-ranged interactions (like electrostatic, hydrophobic, or dispersion) with respect to short-ranged ones (like H-bonds), in order to avoid too sticky interactions that would slow down the reactant mobility substantially due to activated hopping.

Our analytical treatment breaks down if one wishes to push the nanoreactor performances towards full efficiency ($f \rightarrow 1$), where the loading number of NP increases rapidly, or in the

case of larger core sizes (of the order of the whole spherical assembly). In such cases, the diffusive interaction between NPs can no longer be neglected, as well as the effect of the inert PS core, as diffusive and screening interactions among the different boundaries become important. As a consequence, the full exact solution should be employed to investigate the behavior of the rate and elaborate an optimal design of the composite nanoreactor. Interestingly, we have shown that, as a general situation, increasing both the core and the nanocatalyst sizes either has a rather mild effect on the overall performances, or, more generally, causes a rate-boosting effect, with an increase of the overall rate constant of up to 40 % for values of the core size $R_S/R_0 \gtrsim 0.7$.

Acknowledgments

A

In order to determine the unknown coefficients in the expansions (19), we have to express the solution in the local coordinates on every boundary (the $N+1$ spherical surfaces $\partial\Omega_\alpha$) and at the microgel-bulk interface $\partial\Omega_0$, where we impose the pseudo-continuity conditions for the reactant density field. This can be accomplished by using known addition theorems for spherical harmonics [38,39]. After some lengthy algebra, we obtain the following linear equations

$$\frac{1}{\lambda}A_{gq} + \frac{1}{\lambda}\sum_{\beta=1}^{N}\sum_{n=0}^{q}\sum_{m=-n}^{n}B_{mn}^{\beta}V_{g,q}^{\beta,m,n}\mathbb{I}_{\{g-(q-n)\leq m\leq g+(q-n)\}} - E_{gq} = \delta_{g0}\delta_{q0} \tag{28a}$$

$$-B_{gq}^{\alpha} + \frac{(q-h_\alpha)}{(h_\alpha+q+1)}\sum_{n=0}^{\infty}\sum_{m=-n}^{n}\left(A_{mn}H_{m,n}^{(\alpha,g,q)}\mathbb{I}_{q\leq n} + \sum_{\beta=1,\beta\neq\alpha}^{N}B_{mn}^{\beta}W_{m,n}^{(\alpha,\beta,g,q)}\right) = 0 \tag{28b}$$

$$\zeta\left[\sum_{\beta=1}^{N}\sum_{n=0}^{q}\sum_{m=-n}^{n}B_{mn}^{\beta}V_{g,q}^{\beta,m,n}\mathbb{I}_{\{g-(q-n)\leq m\leq g+(q-n)\}} - \frac{q}{q+1}A_{gq}\right] - E_{gq} = 0 \tag{28c}$$

where $h_1 = 0$, $h_\alpha = h$ for $\alpha > 1$ and we have introduced characteristic functions $\mathbb{I}_{m\in\mathscr{I}} = \{1 \text{ for } m \in \mathscr{I}|0 \text{ otherwise}\}$. Eqs. (28a), (28b), (28c)

hold $\forall\ q \in [0,\infty)$ with $\alpha = 1,2,\ldots,N+1$ and $g = -q,-q+1,\ldots,q-1,q$. The matrices V,H,W read

$$V_{g,q}^{\alpha,m,n} = \frac{(-1)^{q-n+m-g}(q-g)!}{(n-m)!(q-n+m-g)!}\eta_{0\alpha}^{q-n}\chi_{\alpha}^{n+1}Y_{m-g,q-n}(-L_\alpha) \tag{29a}$$

$$H_{m,n}^{(\alpha,g,q)} = \binom{n+m}{q+g}\chi_{\alpha}^{q}\eta_{0\alpha}^{n-q}Y_{m-g,n-q}(L_\alpha) \tag{29b}$$

$$W_{m,n}^{(\alpha,\beta,g,q)} = (-1)^{q+g}\frac{(n-m+q+g)!}{(n-m)!(q+g)!}\eta_{\beta\alpha}^{-(n+q)-1}\chi_{\alpha}^{q}\chi_{\beta}^{n+1}Y_{m-g,n+q}(L_{\beta\alpha}) \tag{29c}$$

where $L_{\alpha\beta} = L_\beta - L_\alpha$ (according to this notation $L_{0\alpha} = L_\alpha$) and

$$\eta_{\alpha\beta} = \eta_{\beta\alpha} = \frac{L_{\alpha\beta}}{R_0} \qquad \chi_\alpha = \frac{R_\alpha}{R_0}. \tag{30}$$

Here, for the sake of coherence, we pose $R_1 = R_S$ (radius of the PS core) and $R_\alpha = a$, for $\alpha > 1$ (radius of the nanocatalysts). The system (28a), (28b), (28c) can be expressed more conve-

$$\left(\frac{1}{\lambda}+\frac{q}{q+1}\zeta\right)A_{gq}+\left(\frac{1}{\lambda}-\zeta\right)\sum_{\beta=1}^{N}\sum_{n=0}^{q}\sum_{m=-n}^{n}B_{mn}^{\beta}V_{g,q}^{\beta,m,n}\mathbb{I}_{\{g-(q-n)\leq m\leq g+(q-n)\}}=\delta_{g0}\delta_{q0} \tag{31a}$$

$$-B_{gq}^{\alpha}+\frac{(q-h_{\alpha})}{(h_{\alpha}+q+1)}\sum_{n=0}^{\infty}\sum_{m=-n}^{n}\left(A_{mn}H_{m,n}^{(\alpha,g,q)}\mathbb{I}_{q\leq n}+\sum_{\beta=1,\beta\neq\alpha}^{N}B_{mn}^{\beta}W_{m,n}^{(\alpha,\beta,g,q)}\right)=0 \tag{31b}$$

niently by subtracting eq. (28c) from eq. (28a), which leads to

If the multipole expansions are truncated at N_M multipoles, the system (31)) comprises $(N+2)(N_M+1)^2$ equations, which can be easily solved numerically. Once the the coefficients have been determined, the rate constant can be obtained from eq. (15). Recalling the definitions (19) and making use of

known properties of solid spherical harmonics, it is easy to see that

$$k = -k_S^+ \sum_{\alpha=2}^{N+1} B_{00}^\alpha \qquad (32)$$

The system to be solved has the following structure

$$
\begin{bmatrix}
\left(\frac{1}{\lambda} + \frac{\zeta q}{q+1}\right)\mathbb{I} & \left(\frac{1}{\lambda}-\zeta\right)V^1 & \left(\frac{1}{\lambda}-\zeta\right)V^2 & \cdots & \left(\frac{1}{\lambda}-\zeta\right)V^{N+1} \\
H^1 & -\mathbb{I} & W^{1,2} & \cdots & W^{1,N+1} \\
H^2 & W^{2,1} & -\mathbb{I} & \cdots & W^{2,N+1} \\
\vdots & \vdots & \vdots & \ddots & \vdots \\
H^{N+1} & W^{N+1,1} & W^{N+1,2} & \cdots & -\mathbb{I}
\end{bmatrix}
\times
\begin{bmatrix}
A_{00} \\ \vdots \\ A_{N_M N_M} \\ B_{00}^1 \\ \vdots \\ B_{N_M N_M}^1 \\ \vdots \\ B_{00}^{N+1} \\ \vdots \\ B_{N_M N_M}^{N+1}
\end{bmatrix}
=
\begin{bmatrix}
1 \\ \vdots \\ 0 \\ 0 \\ \vdots \\ 0 \\ \vdots \\ 0 \\ \vdots \\ 0
\end{bmatrix}
$$

To solve this system of equation numerically we employ standard linear algebra packages (LAPACK). The number of multipoles N_M considered to truncate the system was chosen so that the relative accuracy on the rate was less than or equal to $TOL = 10^{-3}$, namely $|k(N_M+1) - k(N_M)|/k(N_M) < TOL$.

B

The monopole approximation of the system (31) for a given configuration of the nanocatalysts can be obtained by truncating the expansion to $q = n = 0$. The ensuing equations read

$$
\begin{cases}
\dfrac{A_{00}}{\lambda} + \left(\dfrac{1}{\lambda}-\zeta\right)\sum_{\beta=1}^N B_{00}^\beta V_{00}^{\beta 00} = 1 \\
B_{00}^\alpha + \dfrac{h_\alpha}{1+h_\alpha}\left(A_{00}H_{00}^{(\alpha 00)} + \sum_{\beta \neq \alpha=1}^N B_{00}^\beta W_{00}^{(\alpha\beta 00)}\right) = 0
\end{cases}
\tag{33}
$$

with $\alpha = 1,2,\ldots,N$. Recalling the definitions (29a), (29b) and (29c), we have $V_{00}^{\beta 00} = a/R_0$, $H_{00}^{(\beta 00)} = 1$, $W_{00}^{(\alpha\beta 00)} = $

$a/L_{\beta\alpha}$, and $\zeta = D_i/D_0$, so that Eqs. (33) take the following form

$$
\begin{cases}
\dfrac{A_{00}}{\lambda} + \dfrac{a}{R_0}\left(\dfrac{1}{\lambda}-\zeta\right)\sum_{\beta=1}^N B_{00}^\beta = 1 \\
B_{00}^\alpha + \dfrac{h_\alpha}{1+h_\alpha}\left(A_{00} + \sum_{\beta\neq\alpha=1}^N B_{00}^\beta \dfrac{a}{L_{\alpha\beta}}\right) = 0
\end{cases}
\tag{34}
$$

Since $B_{00}^\alpha = -k_\alpha/k_S^+$, the overall rate constant of the nanoreactor can be computed simply as $k = -k_S^+ \sum_{\beta=1}^{N+1} B_{00}^\beta$ (note that $B_{00}^1 = 0$ is identically zero as the PS core is modeled as a reflecting sphere). Moreover, we can average the system (34) over the catalyst configurations, in the reasonable hypothesis that spatial correlations between the positions of the catalysts are negligible. This reduces the many-body average to a two-body problem, namely

$$\left\langle \frac{a}{L_{\alpha\beta}} \right\rangle = \frac{9a}{2[(R_0-a)^3-(R_S+a)^3]^2} \int_{R_S+a}^{R_0-a} r^2\,dr \int_{R_S+a}^{R_0-a} \rho^2\,d\rho \int_0^\pi \frac{\sin\theta}{\sqrt{r^2+\rho^2-2r\rho\cos\theta}}\,d\theta$$

$$= \frac{2(1-\varepsilon)^5-5(1-\varepsilon)^2(\gamma+\varepsilon)^3+3(\gamma+\varepsilon)^5}{(1-\varepsilon)^6-2(1-\varepsilon)^3(\gamma+\varepsilon)^3+(\gamma+\varepsilon)^6}\left(\frac{3a}{5R_0}\right) := \varepsilon\, C(\varepsilon,\gamma) \qquad (35)$$

where $\gamma = R_S/R_0$. We therefore get from Eqs. (34)

$$\begin{cases} \dfrac{A_{00}}{\lambda} - \dfrac{a}{R_0}\left(\dfrac{1}{\lambda}-\zeta\right)\dfrac{k}{k_S^+} = 1 \\[2ex] k - \dfrac{h}{1+h}\left[NA_{00}k_S^+ - (N-1)k\left\langle\dfrac{a}{L_{\alpha\beta}}\right\rangle\right] = 0 \end{cases} \qquad (36)$$

where we have taken $h_\alpha = h = k^*/k_S^+ \;\; \forall\; \alpha$ as the N catalysts are identical. By eliminating A_{00} the solution (21) is easily recovered as

$$\frac{k}{k_S^-} = \zeta\,\varepsilon\left(\frac{k}{k_S^+}\right) \qquad (37)$$

The diffusion-limited solution (24) follows straightforwardly in the limit $h \to \infty$.

References

1 V. V. Pushkarev, Z. Zhu, K. An, A. Hervier and G. A. So-morjai, *Topics in Catalysis*, 2012, **55**, 1257–1275.

2 Y. Zhang, X. Cui, F. Shi and Y. Deng, *Chemical Reviews*, 2012, **112**, 2467–2505.

3 M. Haruta, *Chemical Record*, 2003, **3**, 75–87.

4 G. J. Hutchings and M. Haruta, *Applied Catalysis A: General*, 2005, **291**, 2–5.

5 R. M. Crooks, M. Zhao, L. Sun, V. Chechik and L. K. Yeung, *Accounts of Chemical Research*, 2001, **34**, 181–190.

6 J.-H. Noh and R. Meijboom, *Applied Catalysis A: General*, 2015, **497**, 107–120.

7 M. Ballauff, *Progress in Polymer Science*, 2007, **32**, 1135–1151.

8 Y. Lu and M. Ballauff, *Progress in Polymer Science (Oxford)*, 2011, **36**, 767–792.

9 Y. Lu, Y. Mei, M. Drechsler and M. Ballauff, *Angewandte Chemie - International Edition*, 2006, **45**, 813–816.

10 S. Carregal-Romero, N. J. Buurma, J. Perez-Juste, L. M. Liz-Marzan and P. Herves, *Chem. Mater.*, 2010, **22**, 3051–3059.

11 S. Wu, J. Dzubiella, J. Kaiser, M. Drechsler, X. Guo, M. Ballauff and Y. Lu, *Angewandte Chemie - International Edition*, 2012, **51**, 2229–2233.

12 S. Angioletti-Uberti, Y. Lu, M. Ballauff and J. Dzubiella, *The Journal of Physical Chemistry C*, 2015, **119**, 15723–15730.

13 P. Debye, *Trans. Electrochem. Soc.*, 1942, **92**, 265–272.

14 S. Shi, Q. Wang, T. Wang, S. Ren, Y. Gao and N. Wang, *The journal of physical chemistry B*, 2014, **118**, 7177–86.

15 T. Aditya, A. Pal and T. Pal, *Chemical communications (Cambridge, England)*, 2015, **51**, 9410–31.

16 P. Zhao, X. Feng, D. Huang, G. Yang and D. Astruc, *Coordination Chemistry Reviews*, 2015, **287**, 114–136.

17 P. Herves, M. Pérez-Lorenzo, L. M. Liz-Marzán, J. Dzubiella, Y. Lu, M. Ballauff, P. Hervés, M. Pérez-Lorenzo, L. M. Liz-Marzán, J. Dzubiella, Y. Lu and M. Ballauff, *Chemical Society Reviews*, 2012, **41**, 5577.

18 S. Gu, S. Wunder, Y. Lu, M. Ballauff, R. Fenger, K. Rademann, B. Jaquet and A. Zaccone, *The Journal of Physical Chemistry C*, 2014, **118**, 18618–18625.

19 N. Welsch, A. L. Becker, J. Dzubiella and M. Ballauff, *Soft Matter*, 2012, **8**, 1428.

20 D. F. Calef and J. M. Deutch, *Annual Review of Physical Chemistry*, 1983, **34**, 493–524.

21 *Diffusion-limited reactions*, ed. S. A. Rice, Elsevier, Amsterdam, 1985, vol. 25.

22 A. Szabo, *The Journal of Physical Chemistry*, 1989, **93**, 6929–6939.

23 H. X. Zhou, G. Rivas and A. P. Minton, *Annual review of biophysics*, 2008, **37**, 375–397.

24 M. von Smoluchowski, *Physik Z*, 1916, **17**, 557–571.

25 F. C. Collins and G. E. Kimball, *Journal of Colloid Science*, 1949, **4**, 425–437.

26 J. M. Deutch, B. U. Felderhof and M. J. Saxton, *The Journal of Chemical Physics*, 1976, **64**, 4559.

27 B. U. Felderhof and J. M. Deutch, *The Journal of Chemical Physics*, 1976, **64**, 4551.

28 S. D. Traytak, *Chemical Physics Letters*, 1992, **197**, 247 – 254.

29 S. D. Traytak, *The Journal of Composite Mechanics And Design*, 2003, **9**, 495–521.

30 E. Gordeliy, S. L. Crouch and S. G. Mogilevskaya, *International Journal for Numerical Methods in Engineering*, 2009, **77**, 751–775.

31 M. Galanti, D. Fanelli, S. D. Traytak and F. Piazza, *Phys.*

Chem. Chem. Phys., 2016, **18**, 15950–15954.

32 R. Cukier, *Macromolecules*, 1984, **17**, 252–255.

33 O. A. Ladyzhenskaya and N. N. Uralt'seva, *Linear and Quasilinear Elliptic Equations*, Academic Press, New York and London, 1968, vol. 46.

34 Y. Mei, Y. Lu, F. Polzer, M. Ballauff and M. Drechsler, *Chemistry of Materials*, 2007, **19**, 1062–1069.

35 C. Yigit, N. Welsch, M. Ballauff and J. Dzubiella, *Langmuir*, 2012, **28**, 14373–14385.

36 M. Palasis and S. H. Gehrke, *Journal of Controlled Release*, 1992, **18**, 1–11.

37 M. Galanti, D. Fanelli and F. Piazza, 2015, 5.

38 G. Arfken, H. J. Weber and F. E. Harris, *Mathematical Methods for Physicists, Sixth Edition: A Comprehensive Guide*, Elsevier Academic Press, 2005.

39 M. J. Caola, *Journal of Physics A: Mathematical and General*, 2001, **11**, L23–L25.